dc voltage step-up transformer based on a bilayer $\nu=1$ quantum Hall system

B. I. Halperin,[1] Ady Stern,[2] and S. M. Girvin[3]
[1]*Department of Physics, Harvard University, Cambridge, Massachusetts 02138, USA*
[2]*Department of Condensed Matter Physics, Weizmann Institute of Science, Rehovot 76100, Israel*
[3]*Sloane Physics Laboratory, Yale University, P.O. Box 208120, New Haven, Connecticut 06520-8120, USA*
(Received 23 January 2003; published 17 June 2003)

A bilayer electron system in a strong magnetic field at low temperatures, with total Landau-level filling factor $\nu=1$, can enter a strongly coupled phase, known as the (111) phase or the quantum Hall pseudospin ferromagnet. In this phase there is a large quantized Hall drag resistivity between the layers. Here we consider structures where the regions of (111) phase are separated by regions in which one of the layers is depleted by means of a gate, and various of the regions are connected together by wired contacts. We note that with suitable designs, one can create a dc step-up transformer where the output voltage is larger than the input, and we show how to analyze the current flows and voltages in such devices.

DOI: 10.1103/PhysRevB.67.235313 PACS number(s): 73.43.Lp, 73.40.−c, 85.30.−z

I. INTRODUCTION

Following earlier theoretical predictions,[1–5] recent experiments have revealed[6] a unique behavior of coupled electronic transport in a bilayer electronic system in the quantum Hall regime, when the two layers have a total Landau-level filling factor $\nu=1$ (each layer separately being at $\nu\approx 1/2$). If the separation between the layers is sufficiently small, relative to the distance between electrons in a layer, the system can enter a strongly coupled state at low temperatures known as the (111) or quantum Hall pseudospin-ferromagnet phase.[2,7–10] It was predicted for this phase, that if there is no tunneling between the layers, and a current I is driven in one of the layers (the ''active layer''), with no net current flowing in the other (''passive'') layer, then the voltage drop should be identical in the two layers. In the limit of zero temperature, this voltage drop should be purely perpendicular to the current, and equal to Ih/e^2 in each layer. Experiments have confirmed this quantization of the Hall drag resistance with an accuracy of order 10^{-3}.

The properties of the (111) phase reflect a striking form of interlayer phase coherence, which may be understood as a kind of superfluidity in the difference of the electric currents in the two layers, and which shorts out any differences in the electric fields within the two layers.[1–5] The coherent state has a broken symmetry that leads to a Goldstone collective mode[11] and to a giant zero-bias anomaly in the interlayer tunneling spectrum,[12–15] which have both been observed experimentally by Eisenstein and co-workers.[16,17]

In this work we use this equality of the Hall voltage between the two layers to show that a properly constructed bilayer system, incorporating regions of the (111) phase separated by regions where one of the layers is depleted, may serve as a dc voltage step-up transformer.[18] More generally, we show how to analyze the current flows and voltages in devices made up of alternating regions containing the (111) phase and regions where one or the other layer is depleted by a top or bottom gate. We assume throughout that there is no tunneling between the two layers, either because the barrier is too high, or because tunneling has been suppressed by the application of a parallel magnetic field.

In 1965 Ivar Giaver realized a 1:1 dc transformer using flux flow resistance in magnetically coupled superconducting layers.[19] In quantum Hall effect bilayers the layer coupling is of electrostatic origin but the transformer action can be viewed within the composite boson picture as arising from the flow of Chern-Simons flux attached to the particles. In the case of a superconductor, flux flow is mostly perpendicular to the current flow. In the present case the Chern-Simons flux is attached to the particles themselves and flows with them, inducing a voltage drop in the secondary perpendicular to the current flow in the primary.[5]

The proof of the concept is most simply seen in the geometry of Fig. 1, where the upper active layer is used as the primary circuit, with N primary strips in parallel. A time-independent voltage V_1 will lead to a time-independent current I_1 in each of the strips, and this current is independent of N. The voltage across the passive layer, which acts as a secondary circuit, will be $V_2=NI_1h/e^2$ when no current is drawn. Clearly, we will have V_2 larger than V_1 if N is sufficiently large. As we show below, the output impedance of the transformer is nonzero, so that if a nonzero current I_2 is drawn from the secondary, the ratio of the secondary to the

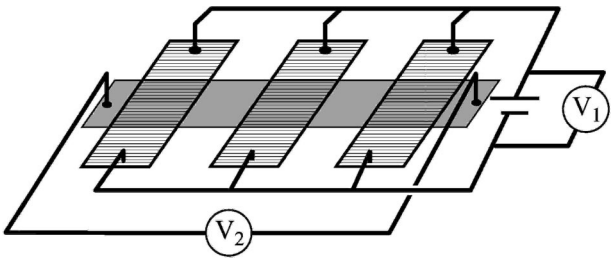

FIG. 1. One version of the transformer, with $N=3$ stages. Horizontal stripes indicate regions where the upper layer is occupied; shading indicates regions where the lower layer is occupied. Areas with both stripes and shading have both layers occupied, with the system in the strongly coupled (111) phase at total Landau-level filling $\nu=1$. The upper layer, divided into strips connected in parallel, is used as the primary. If current I_1 flows in each strip, then a voltage $V_2=NI_1h/e^2$ is induced in the secondary layer, provided no current is drawn.

 ©2003 The American Physical Society

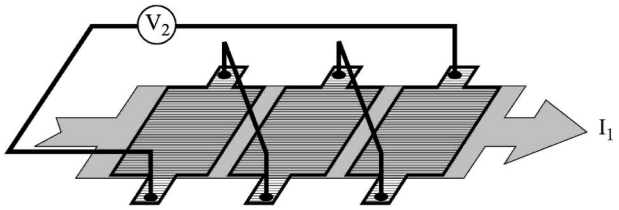

FIG. 2. Alternate version of the transformer. Here the lower layer is used as the primary, while the upper layer, divided into strips connected in series, is used as the secondary.

primary voltage, V_2/V_1, will decrease. If the current I_1 is held fixed and the drawn current I_2 is increased, the secondary voltage V_2 will decrease, and the primary voltage V_1 will increase. Nevertheless, if I_2 is sufficiently small, the secondary voltage will remain larger than the primary.

Another possible geometry, having the strips connected in series rather than in parallel, is illustrated in Fig. 2. A time-independent current I_1 flows in the primary layer, denoted layer 1. This current is driven by a battery with voltage V_1. The voltage V_2 measured in the secondary circuit, when no current is drawn, is equal to NI_1h/e^2 for an N-stage device. (Again, the voltage will be reduced when finite current is drawn from the secondary.) In this case, the voltage V_1 in the primary circuit is also proportional to N. However, we show below that with proper design, the voltage drop V_1 will be smaller than V_2, so that voltage gain is achieved. By connecting together several devices, with a the secondaries in series and the primaries in parallel, one can obtain an arbitrarily large multiplication factor for the voltage.

The structures we discuss are inherently nonuniform, since one of the layers is depleted in parts of the sample. As a consequence, the analysis of current flows and voltage drops is nontrivial. Below, we shall first carry out such an analysis for the case where no current is drawn from the secondary, and then consider the case where $I_2 \neq 0$. We will mostly analyze the device shown in Fig. 2, and discuss the device in Fig. 1 toward the end of the paper. We confine ourselves to the situation where the dimensions of the transformer are large compared to any relevant microscopic length, including the mean free path of any charge carriers. We can then use macroscopic conductivity laws and Kirchoff's equations to determine the current flows and voltage drops in each layer. It is important to distinguish between the classical and quantum aspects of our calculation: the striking transport properties of the (111) phase, particularly the existence of a Hall voltage in a layer where no current is flowing, are a consequence of the quantum Hall effect. In contrast, the nonuniform current distribution we find in some of the regimes we consider, and particularly the confinement of dissipation to ''hot spots,'' is a consequence of the classical Kirchoff's laws for nonuniform systems in a magnetic field.

II. RESISTANCES AND CURRENT FLOWS

Let us define R_N as the ratio V_1/I_1 for an N-stage device of the type shown in Fig. 2, when no current is drawn from the secondary. In the limit where N is large, we can ignore end effects, and write $R_N = NR^*$, where R^* is a constant,

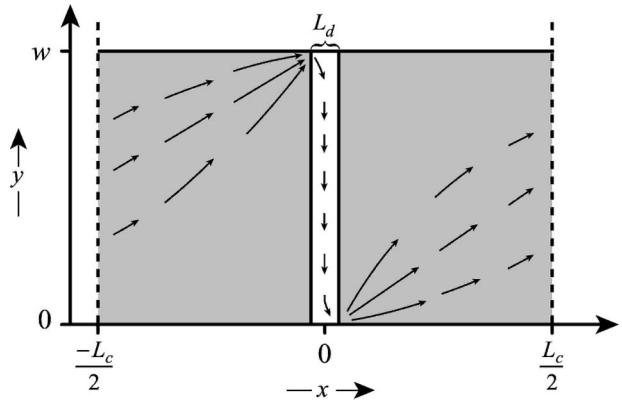

FIG. 3. Schematic unit cell of the device shown in Fig. 2 lies between vertical dotted lines at $x = \pm L_c/2$. Shaded region contains the (111) phase, where both layers are occupied; unshaded region between lines at $x = \pm L_d/2$ has the upper layer depleted. Arrows suggest the flow pattern of an ''extra'' inhomogeneous current, resulting from the y-direction current in the depleted region. To this must be added a uniform current in the x direction, so that the total current is I_1. The inhomogeneous current is small compared to the uniform current in regime (i), $L_d/w \ll \epsilon$, where $\epsilon h/e^2$ is the longitudinal resistivity in the depleted region.

assuming that all intermediate stages are identical to each other. The value of R^* can be calculated by considering an infinite periodic system, with the unit cell shown in Fig. 3. The primary layer occupies a region of width w running parallel to the x axis, which we label $0 < y < w$. The secondary layer is depleted in a short region, of length L_d, which we take here to be region $-L_d/2 < x < L_d/2$. In the remainder of the unit cell, of total length L_c, both layers are occupied, and the system is in the (111) phase. We have assumed that the voltage tabs attached to the secondary layer shown in Fig. 2 are narrow, so they do not perturb the current flow when no net current is drawn from the voltage contacts. Thus there is no current flow in either layer across the boundaries at $y = 0$ and $y = w$.

We assume that in the parts of the sample where one of the layers is depleted, the other layer (whose filling factor is $\approx 1/2$) is in a compressible state, characterized by a resistivity tensor ρ^1 with

$$\rho^1_{yx} = -\rho^1_{xy} \equiv \nu_1^{-1} \approx 2, \tag{1}$$

$$\rho^1_{xx} = \rho^1_{yy} \equiv \epsilon \ll 1. \tag{2}$$

We have chosen the magnetic-field direction along the positive z axis, so that ρ^1_{yx} is positive, and we use units where $h/e^2 = 1$ for intermediate steps of the calculation. In the coherent (111) region, where both layers are occupied, there is no resistivity to a flow of an antisymmetric current. For a symmetric current, the Hall resistivity is quantized $\rho^{\rm coh}_{yx} = -\rho^{\rm coh}_{xy} = 1$. The diagonal resistivity vanishes rapidly at low temperatures and we take it here to be a negligibly small, but non-zero, positive quantity. We carry out our analysis of the current flow patterns assuming that the diagonal resistivities in each of the two phases do not fluctuate

with position. However, our results for the operation of the device as a dc voltage step-up transformer are independent of that assumption.

Let $\mathbf{j}^{\alpha}(\mathbf{r})$ and $\phi^{\alpha}(\mathbf{r})$ be the current density and the potential in layer α, and $\mathbf{E}^{\alpha}=-\boldsymbol{\nabla}\phi^{\alpha}$ be the electric field in layer α. In the geometry of Fig. 2 no current flows in the secondary layer, i.e., $\mathbf{j}^2=0$. This is obviously true in the regions where this layer is depleted, but in fact, holds also in the coherent (111) regions. In these regions, the superfluidity shorts out any antisymmetric electric fields, so $\mathbf{E}^1=\mathbf{E}^2$, and the potentials in the two layers differ only by a constant. The antisymmetric current in the coherent region, $\mathbf{j}^1-\mathbf{j}^2$, is a supercurrent, so its curl and divergence both vanish.[20] In fact, the same holds for the total (symmetric) current: the divergence $\boldsymbol{\nabla}\cdot(\mathbf{j}^1+\mathbf{j}^2)=0$ due to current conservation, and the curl vanishes since $\boldsymbol{\nabla}\times\mathbf{E}^1=0$ and the resistivities in the (111) phase are independent of position. Thus the values of both $\mathbf{j}^1,\mathbf{j}^2$ in the coherent regions are determined by the boundary conditions: their normal component must vanish at the top and bottom edges, $y=0$ and $y=w$, while the normal component of $\mathbf{j}^2$ must vanish also at the boundaries between the coherent and depleted regions. Thus, current $\mathbf{j}^2$ vanishes everywhere, and no current flows in the secondary layer.

The current distribution $\mathbf{j}^1$ in the active layer may be analyzed by solving Kirchoff's equations. It is useful to define a ''reduced potential'' $V(\mathbf{r})$ by

$$\boldsymbol{\nabla}\phi^1=\boldsymbol{\nabla}V-\hat{z}\times\mathbf{j}^1. \tag{3}$$

$V(\mathbf{r})$ is the potential corresponding to a current density $\mathbf{j}^1(\mathbf{r})$ in a system where the coherent regions are superfluids for *both* symmetric and antisymmetric currents, and where the depleted regions have a Hall resistivity of $\nu_1^{-1}-1$ rather than ν_1^{-1}. Within the depleted region

$$\nabla^2 V=0, \tag{4}$$

and four boundary conditions should be imposed. The first two are

$$\epsilon\partial_x V+(1-\nu_1^{-1})\partial_y V=0 \quad \text{at} \quad y=0 \text{ and } y=w, \tag{5}$$

which assure that the current at the edges is parallel to the edges. The other two,

$$V(x,y)=V_0 \quad \text{at} \quad x=-\frac{L_d}{2}, \tag{6}$$

$$V(x,y)=0 \quad \text{at} \quad x=\frac{L_d}{2}, \tag{7}$$

result from the vanishing longitudinal resistivity at the (111) region. The value of V_0 is proportional to I_1, and should be chosen such that

$$\int_0^w dy\, j_x^1=I_1, \tag{8}$$

where the current density is given by

$$\mathbf{j}^1(\mathbf{r})=\frac{\nu_1^{-1}-1}{\epsilon^2+(1-\nu_1^{-1})^2}\hat{z}\times\boldsymbol{\nabla}V-\frac{\epsilon}{\epsilon^2+(1-\nu_1^{-1})^2}\boldsymbol{\nabla}V. \tag{9}$$

The integral in Eq. (8) may be taken at any convenient value of x. Having defined the equation and boundary conditions for $V(r)$, we notice that $V(r)$ is the potential generated by a capacitor subject to voltage V_0 and to unusual boundary conditions at the edges.

As we now show, there are three different regimes for this problem, according to the ratio of the two dimensionless parameters in our definition of the problem, the aspect ratio L_d/w and the longitudinal resistivity ϵ. The regimes are (i) $L_d/w\ll\epsilon$, (ii) $\epsilon\ll L_d/w\ll 1/\epsilon$, and (iii) $1/\epsilon\ll L_d/w$.

A. Regime (i): $L_d/w\ll\epsilon$

We start with the first regime. When $L_d/w\to 0$, the system is very wide and the edges may be neglected. Far from the edges j_x^1, E_y^1 are independent of position. They are then equal to I_1/w, both in the (111) region and in the depleted region, while $\partial_y V$ vanishes. In the (111) region, the electric field is purely perpendicular to the current, but this is not true in the depleted region, where the longitudinal resistivity is nonzero. Substituting these values of j_x^1, E_y^1 in the relation $\mathbf{E}=\rho^1\mathbf{j}$ we obtain

$$j_y^1=\nu_1\left[\epsilon\frac{I_1}{w}-E_x^1\right]=\frac{I_1}{w}\frac{1-\nu_1^{-1}}{\epsilon}, \tag{10}$$

$$E_x^1=\frac{I_1}{w}\left\{\epsilon-\frac{1-\nu_1^{-1}}{\nu_1\epsilon}\right\}, \tag{11}$$

and $V_0=E_x^1 d$. These results apply throughout the depleted region, except for small regions, with dimensions of order L_d, close to the top and bottom edges, at $y=0$ and $y=w$. (See Sec. II C, below.) The integrated current $I_y^1=L_d j_y^1$ leaves the depleted region near $y=0$, and spreads out into the (111) region, where it eventually flows up towards the upper edge and back into the depleted region near $y=w$. This extra current flow is shown by arrows in Fig. 3. The integrated current flow across the midline $y=w/2$ in the (111) region, must be exactly equal and opposite to the integrated vertical current I_y^1 in the depleted region, as there can be no net current flow in the y direction. Since a current density j_y at a point in the (111) region must be driven by a Hall electric field in the x direction, we see that $\int E_x^1 dx$ along the midline of a (111) region, say from the point $x=L_d/2$ to the point $x=L_c-L_d/2$, must be equal to I_y^1. Adding in the contribution from the field E_x in the depleted region, we see that the total voltage drop along the midline of a unit cell, say from the point $x=-L_d/2$ to $x=L_c-L_d/2$, is equal to $I_1 R^*$, with

$$R^*=\frac{L_d}{w\epsilon}[(1-\nu_1^{-1})^2+\epsilon^2]. \tag{12}$$

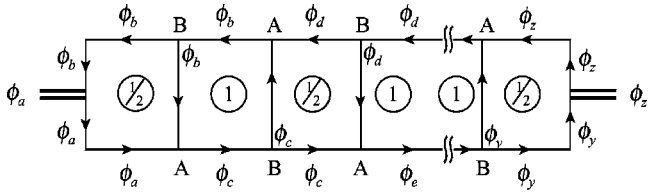

FIG. 4. Network model when there is no dissipation in the interior of the sample. Lines with arrows are bonds, with orientation as described in the text. Double lines are metallic leads. Numbers in circles denote the Hall conductivity σ_{xy} (in units of e^2/h) within each region. Potentials on the bonds, in the primary layer 1, and on the leads, are denoted by ϕ_a, ϕ_b, etc. Dissipation occurs at nodes labeled *A* and at the contacts to the leads.

We see that R^* can be made arbitrarily small by using a sample with a large width w, and by making the length L_d of depleted region as small as possible.

Since there is no current flow across the edges at $y=0$ and $y=w$, we see that E_x^1 and E_x^2 both vanish along these edges in the (111) regions. Potentials ϕ^α are therefore constants along each of these edges, in a given (111) region, and the potential difference between $y=0$ and $y=w$ in a given layer is just the Hall voltage, I_1. The difference in potential between layer 1 and layer 2 is an arbitrary constant that has no effect on the current flows or voltage drops along the layers. Thus, if the edges of the secondary layer are connected together as shown in Fig. 2, and no current is drawn from the secondary circuit, we obtain $V_2 = NI_1 h/e^2$ as claimed in the Introduction.

B. Regime (ii): $\epsilon \ll L_d/w \ll \epsilon^{-1}$

Naively, one might expect the analysis above to hold as long as $L_d \ll w$, but, in fact this is not the case. As often happens at the interface of materials with different Hall resistivities in the regime of strong magnetic fields, the current distribution can become very inhomogeneous, when the Hall angle is large, and this can have a major effect on the voltage drop (see, e.g., Ref. 21, and references therein). However, the analysis again becomes simple in regime (ii), where ϵ is small compared to both L_d/w and w/L_d. We can understand this regime by taking the limit $\epsilon \to 0$ with L_d and w fixed. In this case the boundary conditions (5)–(7) imply that the reduced potential $V(x,y)$ is a constant along each boundary of the depleted region, with the exception of two hot spots, at corners where two boundaries meet. At these corners, there is a discontinuity in V, or more accurately, a very rapid change of the potential, on a length scale of order ϵL_d. In the limit $\epsilon \to 0$, the resulting divergence of the electric field leads to a finite total current crossing the boundary between the (111) region and the depleted region in the corner, with a finite amount of dissipation. Everywhere other than at the corner hot spots the electric fields remain finite and, thus, there is no dissipation other than at these corners.

The voltage drop in regime (ii) can be calculated using a simple network model, illustrated in Fig. 4. (The hot spots where dissipation takes place are marked *A* in this figure.) The boundaries between different Hall regions, or between a Hall region and the vacuum, are represented by bonds in the model. Each bond is assigned a directional arrow, oriented so that the Hall conductance $\sigma_{xy} = 1/\rho_{yx}$ of the region on the left-hand side of the bond is algebraically larger than the Hall conductance on the right. (An insulating region is assigned a Hall conductance $\sigma_{xy} = 0$.) For each bond μ, we denote the absolute value of the difference in these Hall conductivities by $\sigma_\mu > 0$. Note that if one were to reverse the sign of the magnetic field, the signs of the Hall conductances would change, as would the directions of the arrows, but σ_μ would be unchanged.

Let ϕ_μ denote the potential ϕ^1 on bond μ, which is a constant along the length of the bond. In the network model, the bond carries a current $i_\mu = \sigma_\mu \phi_\mu$, and an energy flux $i_\mu \phi_\mu$, with positive signs denoting transport in the direction of the arrow. Although the current flow in the original problem is not actually confined to the edges and boundaries, the details of the flow are irrelevant to a computation of the voltage drop along the edges. The voltage difference between any two points on the boundaries of a given Hall region is completely determined by the total Hall current crossing a line joining the two points, if the diagonal resistivity is zero. Thus there is no error introduced by associating the currents with the boundaries.

Nodes in the network, where three bonds come together, represent the meeting point of three Hall regions. Current conservation requires that the current leaving a node must equal the current entering, while energy conservation dictates that the energy flux leaving the node be equal to or smaller than the energy entering. There are two types of nodes. When there are two bonds with arrows pointing into the node (labeled $\mu = 1,2$), and one pointing out (labeled $\mu = 3$), then the potentials on the incoming bonds are arbitrary, and the potential on the outgoing bond is determined by current conservation:

$$\phi_3 = (\phi_1 \sigma_1 + \phi_2 \sigma_2)/\sigma_3, \tag{13}$$

with $\sigma_3 = \sigma_1 + \sigma_2$. On the other hand, for a node with one incoming bond and two outgoing bonds, the requirements of current and energy conservation dictate that the potentials on the outgoing bonds be equal to the potential on the incoming bond.

In addition to the nodes described above, we include additional junctions to represent an Ohmic contact with a metallic lead. For an ideal contact, the condition is that the potential on the bond leaving the contact is the same as the voltage in the metallic lead. The potential on the incoming bond is arbitrary. (For a nonideal contact, one may include a series resistance, which leads to an additional voltage drop if there is net current flowing into or out of the lead.)

Using the above rules, we see that the there are no potential differences among the three bonds connected to each of the nodes labeled *B* in Fig. 4. However, there are voltage drops at the nodes marked *A*. If the net current in the x direction is I_1, then we must have $I_1 = \nu_1(\phi_a - \phi_b) = (\phi_c - \phi_b) = \nu_1(\phi_c - \phi_d)$, etc. Then we find $\phi_a - \phi_c = \phi_b - \phi_d = I_1 R^*$, where

$$R^* = (\nu_1^{-1} - 1). \tag{14}$$

C. Crossover between regimes (i) and (ii)

Comparing Eqs. (12) and (14) , we see that the two expressions for R^* become equal when the aspect ratio L_d/w is of order ϵ, suggesting that this is indeed the boundary between regimes (i) and (ii), as claimed. In fact, one can obtain an exact expression for R^* that is valid throughout this crossover regime. To do this, let us consider the problem where both ϵ and the aspect ratio L_d/w are very small, but with arbitrary ratio between them. It is convenient to think of L_d as fixed, with w very large and ϵ very small. As discussed above for the case of regime (ii), the reduced potential V on the lower edge ($y=0$) will be a constant, equal to V_0, except for a small interval, of order $\epsilon L/d$ near the right corner, at $x=L_d/2$, while on the upper edge ($y=w$) we have $V=0$ except for a small interval near the left corner, at $x=-L_d/2$.

We may solve Eqs. (4), (6), and (7) by writing

$$V(x,y) = V_0 - \frac{xV_0}{L_d} + \sum_n (A_n e^{-k_n y} + B_n e^{k_n y}) \times \sin k_n (x + L_d/2), \tag{15}$$

where n is summed over positive integers and $k_n = \pi n/L_d$. The coefficients A_n, B_n are determined by the values of V at $y=0$ and $y=L$. We see that as long as $n \ll \epsilon^{-1}$, one has

$$A_n \approx -\frac{V_0}{\pi n}(-1)^n,$$

$$B_n \approx -\frac{V_0}{\pi n} e^{-k_n w}. \tag{16}$$

For $n > \epsilon^{-1}$, the coefficients fall off more rapidly than $1/n$.

The total current flowing in the x direction can be found most conveniently by evaluating integral (8) at the center line, $x=0$. The first term in Eq. (15) gives rise to a "bulk" contribution , $I_x^{\text{bulk}} = (V_0 \epsilon w/L_d)[(1-\nu_1^{-1})^2 + \epsilon^2]^{-2}$, which is the same as that obtained earlier in region (i). The second term in Eq. (15) gives rise to an "edge current," concentrated in regions of order L_d near the upper and lower edges, and falling off exponentially away from these edges. As we are considering the situation where $w \gg L_d$, the edge current is independent of w, and simply adds to the bulk current. In the limit $\epsilon \ll 1$, the edge current is derived entirely from the first term in Eq. (9) (i.e., the Hall term) and it leads to a total contribution $I_x^{\text{edge}} = V_0/(\nu_1^{-1} - 1)$, which is the same as the result in regime (ii).[22] Thus we find, for $\epsilon \ll 1$ and $L_d \ll w$, including the crossover region between regimes (i) and (ii), the resistance R^* of a depleted region is given by

$$\frac{1}{R^*} = \frac{1}{\nu_1^{-1} - 1} + \frac{\epsilon w}{L_d[(1-\nu_1^{-1})^2 + \epsilon^2]} \tag{17}$$

Although the edge current near the center line $x=0$ is spread out over a region of height $\approx L_d$, we note that very close to the interfaces, at $x = \pm L_d/2$, the current is concentrated in a smaller interval, of height $\approx \epsilon L_d$, at the hot-spot corner.

D. Regime (iii) $\epsilon^{-1} \ll L_d/w$

It is clear that the length-independent expression for R^* given by Eq. (14) must break down, if L_d is sufficiently large. When $L_d/w > \epsilon^{-1}$ [regime (iii)], the resistance of each stage is proportional to the longitudinal resistivity of the depleted region, and is given by

$$R^* = \epsilon L_d/w. \tag{18}$$

This regime is of no interest, if we want to create a device with small R^*.

The crossover between regimes (ii) and (iii) may also be solved analytically by considering a depleted region where both ϵ and w/L_d are very small, but with an arbitrary ratio between them. This problem may be solved by a method similar to that used for the crossover between regimes (i) and (ii). In fact, the two problems may be related by a duality transformation, in which the electric fields and the currents are interchanged, and the spatial coordinates are rotated by 90 degrees. The final result now is that resistance R^* is the sum of the results given by Eqs. (14) and (18).

E. Total resistance R_N

Equations (12), (14), and (18) give R^*, the resistance for each of the $(N-1)$ intermediate depleted regions, in the three aspect-ratio regimes. To this we must add the resistance arising from the Ohmic contacts to the depleted end tabs in Fig. 2. If the lengths L_d' of the end tabs are such that the aspect ratio L_d'/w is in the intermediate regime, large compared to ϵ but small compared to ϵ^{-1}, then the resistance of the end tabs may be analyzed using the network model, as illustrated in Fig. 4. We readily find that the combined added resistance of the two end tabs is equal to $2\nu_1^{-1} - 1$. This resistance is composed of ν_1^{-1}, the two-terminal resistance of the depleted system, and $\nu_1^{-1} - 1$, the resistance associated with the interface between the depleted and (111) parts. Thus we find a total resistance in layer 1 of

$$R_N = [(N-1)R^* + (2\nu_1^{-1} - 1)]\frac{h}{e^2} \approx [(N-1)R^* + 3]\frac{h}{e^2}. \tag{19}$$

(Having arrived at the presentation of our final formulas, we now restore the factor of h/e^2.) For a device containing two voltage tabs in regime (ii) and one (111) region ($N=1$), this gives resistance $R_1 \approx 3h/e^2$.

We note then that in order to have $V_2 > V_1$, with the device in Fig. 2, we must choose the aspect ratio L_d/w of the intermediate depleted regions to be smaller than ϵ. For technical reasons, it may be difficult to attach an Ohmic contact to a very short end tab whose length L_d' is smaller than ϵw. On the other hand, it should be possible to fabricate a device where the lengths L_d of the intermediate depleted regions are very short, by using narrow wires as top gates. Although the

additional resistance R^* for each intermediate stage is small compared to h/e^2 in this case, the total resistance cannot be smaller than the value $\approx 3h/e^2$ for a single stage device. From Eq. (19), we see that in order to have a larger voltage in the secondary than in the primary, even for very small values of $L_d/\epsilon w$, the number of stages N must be $\geqslant 4$.

F. Effect of finite current in secondary

We now consider what happens if there is a finite current I_2 drawn from the secondary. The linearity of the circuit means that we can write

$$V_1 = AI_1 + CI_2, \tag{20}$$

$$V_2 = BI_1 - DI_2, \tag{21}$$

where $A = R_N$ and $B = Nh/e^2$ as given above, and C and D are constants to be determined now. If we set $I_1 = 0$ with $I_2 \neq 0$, we have effectively interchanged the roles of the primary and secondary layers. We see from this that $C = Nh/e^2$. Also, if the tabs for the contacts to layer 2 have an aspect ratio between ϵ and ϵ^{-1}, we see that D will be N times the resistance of the primary layer of a single-stage device: $D \approx 3Nh/e^2$. The output impedance of the secondary is appropriately defined as

$$Z = -\left(\frac{\partial V_2}{\partial I_2}\right)_{I_1} = D. \tag{22}$$

If the secondary circuit is closed by a load resistance R, we find

$$\frac{V_2}{V_1} = \frac{BR}{AR + AD + BC}. \tag{23}$$

G. Structure in Fig. 1

Finally we consider the structure shown in Fig. 1, which we may analyze in a manner similar to the above. If the aspect ratios of the depleted regions are all in the intermediate regime $\epsilon < L_d/w < \epsilon^{-1}$, and we define I_1 as the current in *each* primary strip, then we obtain the following results for the constants in Eqs. (20)–(23): $A \approx 3h/e^2, C = h/e^2, B = Nh/e^2, D \approx (N+2)h/e^2$. In this case we obtain a voltage ratio $V_2/V_1 \approx N/3$, which exceeds unity provided $N \geqslant 4$. For large N, the output impedance is lower than that of the geometry in Fig. 2.

III. ADDITIONAL REMARKS

Throughout our analysis, we have assumed that the dimensions of the system are large enough for us to use macroscopic constitutive relations for the current and voltage in each region. For the geometry of Fig. 2, the most critical requirement for our analysis is that the length L_d of the depleted region must be larger than the mean free path of quasiparticles in the single-layer phase, so that a macroscopic resistivity may be used. In general, for a large but finite system, there will be corrections to the macroscopic equations arising from the boundaries between regions, which could either increase or decrease the total resistance. However, the boundary contribution to the resistance should decrease as the reciprocal of the length of the boundary, so that the boundary contribution becomes negligible in the macroscopic limit.

IV. CONCLUSIONS

In summary, in this paper we have considered two possible geometries for a quantum Hall bilayer device, which should be able to act as a dc transformer with voltage gain, and analyzed the current flow patterns in these geometries. In particular, our analysis permits us to calculate the voltage differences between any two points on the edge of the sample, in either layer, given the total current flow in each layer. The methods we have used for this analysis are applicable more generally, to composite systems where all components of the systems are characterized by a longitudinal resistivity much smaller than the Hall resistivity. Finally, experiments to test our proposals for a dc voltage step-up transformer, and to measure the voltage drops in various geometries, would help strengthen our understanding of the interlayer correlations and phase coherence found in strongly coupled $\nu = 1$ bilayer systems.

ACKNOWLEDGMENTS

The authors are grateful to James Eisenstein for several helpful discussions, including comments on the manuscript. This work was supported by NSF Grant Nos. DMR-0196503 (S.M.G.), DMR-DMR-0233773 (B.I.H.), the US-Israel Binational Science Foundation (A.S. and B.I.H), and the Israel Science Foundation (A.S.).

[1] J.M. Duan, Europhys. Lett. **29**, 489 (1995).

[2] K. Moon, H. Mori, Kun Yang, S.M. Girvin, A.H. MacDonald, L. Zheng, D. Yoshioka, and Shou-Cheng Zhang, Phys. Rev. B **51**, 5138 (1995). [Note that transport Eq. (171) contains an erroneous factor of 2 in the denominator.]

[3] Kun Yang, Phys. Rev. B **58**, R4246 (1998), and references therein.

[4] Fei Zhou and Yong Baek Kim, Phys. Rev. B **59**, R7825 (1999).

[5] For a recent review see: S.M. Girvin, in *Proceedings of the Nobel Jubilee Symposium on Condensation & Coherence in Condensed Matter*, edited by Tord Claeson and Per Delsing [Phys. Scr. **T102**, 112 (2002)].

[6] M. Kellogg, I.B. Spielman, J.P. Eisenstein, L.N. Pfeiffer, and K.W. West, Phys. Rev. Lett. **88**, 126804 (2002).

[7] B.I. Halperin, Helv. Phys. Acta **56**, 75 (1983).

[8] *Perspectives in Quantum Hall Effects*, edited by Sankar Das

Sarma and Aron Pinczuk (Wiley, New York, 1997).
[9] S.M. Girvin, in *Topological Aspects of Low Dimensional Systems*, Les Houches Lecture Notes, edited by Alain Comtet, Thierry Jolicoeur, Stephane Ouvry, and Francois David (Springer-Verlag, Berlin/Les Editions de Physique, Les Ulis, 2000); S.M. Girvin, cond-mat/9907002 (unpublished).
[10] K. Yang, K. Moon, L. Belkhir, H. Mori, S.M. Girvin, A.H. MacDonald, L. Zheng, and D. Yoshioka, Phys. Rev. B **54**, 11 644 (1996).
[11] H. Fertig, Phys. Rev. B **40**, 1087 (1989).
[12] Xiao-Gang Wen and A. Zee, Phys. Rev. Lett. **69**, 1811 (1992); Phys. Rev. B **47**, 2265 (1993); Europhys. Lett. **35**, 22 (1996); Z.F. Ezawa and A. Iwazaki, Int. J. Mod. Phys. B **19**, 3205 (1992); Phys. Rev. B **47**, 7295 (1993); Z.F. Ezawa, *ibid.* **51**, 11 152 (1995).
[13] Michael M. Fogler and Frank Wilczek, Phys. Rev. Lett. **86**, 1833 (2001).
[14] L. Balents and L. Radzihovsky Phys. Rev. Lett. **86**, 1825 (2001).
[15] Ady Stern, S.M. Girvin, A.H. MacDonald, and Ning Ma, Phys. Rev. Lett. **86**, 1829 (2001).
[16] I.B. Spielman, J.P. Eisenstein, L.N. Pfeiffer, and K.W. West, Phys. Rev. Lett. **87**, 036803 (2001).
[17] I.B. Spielman I, J.P. Eisenstein, L.N. Pfeiffer, and K.W. West, Phys. Rev. Lett. **84**, 5808 (2000).
[18] Another dc transformer, working also in the quantum Hall regime but based on a very different design, was proposed by D.B. Chklovskii and B.I. Halperin, Phys. Rev. B **57**, 3781 (1998).
[19] Ivar Giaver, Phys. Rev. Lett. **15**, 825 (1965); R. Deltour and M. Tinkham, Phys. Rev. **174**, 478 (1968); J.W. Ekin, B. Serin, and J.R. Clem, Phys. Rev. B **9**, 912 (1974).
[20] Because vortices carry charge, there can be frozen-in vortices that give a curl to the supercurrent, but these fixed circulating currents can be ignored as they do not modify the total transport current.
[21] I.M. Ruzin, Phys. Rev. B **47**, 15 727 (1993).
[22] Taking into account the second term in Eq. (9), we find that the leading correction to the edge current I_x^{edge} is a factor $[1+\epsilon \ln 2/(1-\nu^{-1})\pi]$, in the limit $\epsilon \ll 1$.